NASA Technical Memorandum 87165

Effect of Interference Fits on Roller Bearing Fatigue Life

(NASA-TM-87165) EFFECT ON INTERFERENCE FITS ON ROLLER BEARING FATIGUE LIFE (NASA) 24 p
C A02/MF A01 CSCL 13I

N86-19616

Unclas
G3/37 05177

Harold H. Coe and Erwin V. Zaretsky
Lewis Research Center
Cleveland, Ohio

January 1986

NASA

EFFECT OF INTERFERENCE FITS ON ROLLER BEARING FATIGUE LIFE

Harold H. Coe and Erwin V. Zaretsky
National Aeronautics and Space Administration
Lewis Research Center
Cleveland, Ohio 44135

E-2516

SUMMARY

An analysis was performed to determine the effects of inner-ring speed and press fits on roller bearing fatigue life. The effects of the resultant hoop and radial stresses on the principal stresses were considered. The maximum shear stresses below the Hertzian contact were determined for different conditions of inner ring speed and load, and were applied to a conventional roller bearing life analysis. The effect of mean stress was determined using a Goodman diagram approach. Hoop stresses caused by press fits and centrifugal force can reduce bearing life by as much as 90 percent. Use of a Goodman diagram predicted life reduction of 20 to 30 percent. The depth of the maximum shear stress remained virtually unchanged.

NOMENCLATURE

A	defined by equation (48), N/M^2 ($lb/in.^2$)
B	defined by equation (25) dimensionless
b	semiwidth of contact area (see fig. 1), M (in.)
c	stress-life exponent
E	modulus of elasticity, N/M^2 ($lb/in.^2$)
E'	defined by equation (13), M^2/N ($in.^2/lb$)
e	Weibull slope (exponent)
G	defined by equation (30) dimensionless
g	gravitational constant, M/sec^2 (in/sec^2)
h	exponent
K	defined by equation (30), $N\text{-}sec/M^4$ ($lb\text{-}sec/in^4$)
K_1	constant relating press fit to pressure ($=2/E(1-B^2)$) (for a solid shaft)
K_2	defined by equation (45) dimensionless
K_3	material constant
L	contact fatigue life, hr

LR	life ratio, defined by equation (52)
ℓ	length of contact area (fig. 1), M (in.)
m	defined by equation (48), N/M^2 ($lb/in.^2$)
P_1	pressure on r_1, due to press fit, N/M^2 ($lb/in.^2$)
P_o,	pressure on r_o, N/M^2 ($lb/in.^2$)
P_o'	roller load, N (lb)
R	radius of curvature, M (in.)
R'	ratio, defined by equation (44) dimensionless
R_r	radius of roller (fig. 3), M (in.)
r	radius to element (fig. 3), M (in.)
r_1	ring inner radius (fig. 3), M (in.)
r_o	ring outer radius (fig. 3), M (in.)
S_{max}	Hertz stress at center of contact, N/M^2 ($lb/in.^2$)
Su	ultimate strength of material, N/m^2 ($lb/in.^2$)
Sy	principal stress in the Y-direction (eq. (34)), N/M^2 ($lb/in.^2$)
S_Z	principal stress in the Z-direction (eq. (33)), N/M^2 ($lb/in.^2$)
t	simplifying term ($=\sqrt{1 + u^2}$)
u	dimensionless depth below surface (=Z/b)
V	stressed volume, M^3 ($in.^3$)
X	axis perpendicular to rolling direction
X_X	principal stress, X-direction, Hertz loading only (eq. (4)), N/M^2 ($lb/in.^2$)
Y	axis in direction of rolling
Y_Y	principal stress, Y-direction, Hertz loading only (eq. (5)), N/M^2 ($lb/in.^2$)
y	defined by eq. (25) dimensionless
y_{max}	value of y at τ_{max} dimensionless
Z	distance below Hertz contact surface (fig. 1), M (in.) or axis in direction of Hertzian loading

Z_o value of depth to maximum shearing stress, M (in.)

Z_Z principal stress, Z-direction, Hertz loading only (eq. (6)), N/M^2 ($lb/in.^2$)

γ density of material, N/M^3 ($lb/in.^3$)

Δ press fit on radius, M (in.)

δ Poisson's ratio (also ν) dimensionless

θ defined by eq. (10), N/M^2 ($in.^2/lb$)

Λ defined by eq. (15), M^3/N ($in.^3/lb$)

ν Poisson's ratio (also δ) dimensionless

π P_i (=3.14159)

$\Sigma\rho$ curvature sum (=1/Ra + 1/Rb), 1/M (1/in.)

σ stress, N/M^2 ($lb/in.^2$)

τ maximum shear stress, N/M^2 ($lb/in.^2$)

τ_a amplitude of τ, N/M^2 ($lb/in.^2$)

τ_e effective maximum shear stress, N/M^2 ($lb/in.^2$)

τ_m mean value of τ, N/M^2 ($lb/in.^2$)

τ_{max} maximum value of τ, N/M^2 ($lb/in.^2$)

ω inner ring speed, rad/sec

Subscripts

a body a

b body b

CF due to inner ring speed

H based on Hertz loading only

h hoop- or Y-direction

PF due to press fit on inner ring

T based on press fit and ring speed and Hertz loading

r radial- or Z-direction

INTRODUCTION

With advancements in turbomachinery, rolling-element bearing operating speeds and temperatures have been steadily increasing. Because of centrifugal loading on the bearing inner ring-shaft interface, and differential temperatures, the inner ring expands or grows relative to the shaft. This can result, even in a highly loaded bearing application, in the inner ring "walking" around the shaft. The most benign effect of this phenomenon is replacement of the bearing at overhaul and plating and regrinding of the shaft at the bearing position due to wear. However, in the most extreme cases, the wear of the shaft can either act as a stress raiser to cause fatigue or fracture of the shaft or in the case of hollow shafts actually wear through the shaft. In these cases, catastrophic or secondary damage can occur.

In order to prevent motion of the inner ring around a shaft, designers have been specifying very tight interference fit between the inner ring and shaft where it is not practical to provide for a keyway or locknut arrangement. The interference fit is usually based upon the anticipated growth of the shaft and bearing under the most severe operating conditions. These conditions sometimes only exist for short time periods in the machine's operating cycle. Nevertheless, it is a very important design consideration for both safety of operation as well as maintainability. In recent years it has been noticed by some engineers that bearings which have higher than usual interference or press fits may have field lives which are shorter than those which were anticipated or calculated. The failure mechanism is usually classical rolling-element (subsurface) fatigue. There has been no public documentation of the phenomenon.

Residual compressive stresses near the surface of a rolling element increases the rolling-element fatigue life of the surface under rolling contact loading (refs. 1 to 4). These compressive residual stresses can be developed for a number of processing operations such as grinding and shot peening (ref. 4). Tensile residual stresses while not common can negatively affect fatigue life. These tensile residual stresses would be analogous to those hoop tensile stresses which may be induced due to press fits and ring growth due to thermal and centrifugal effects. If residual stress can affect the fatigue life, then these other stresses which can be present may also alter the critical subsurface shearing stress and affect rolling-element fatigue life of the bearing inner race.

Czyzewski (ref. 5) first postulated that tensile stresses in a cylindrical race imposed on a lubricated Hertzian contact would affect shearing stresses and, hence, rolling-element fatigue life. He performed an analysis and rolling-element fatigue tests of 45-mm bore roller bearing inner-races subjected to mechanically induced tensile stress. Maximum Hertzian stress was approximately 700 MN/m^2 (102×10^3 psi). There is a suggestion of an inverse ninth power stress-life relation. At a hoop tensile stress of 80 MN/m^2 (12×10^3 psi) failure appears to be by a surface fatigue spall accompanied by ring fracture. At the lower hoop stresses, the failure mode was by classical rolling-element fatigue.

The research reported herein was undertaken to investigate the effects of inner-ring press fits and centrifugal force on roller bearing life. The objectives were (a) develop an equation to account for the effect of hoop stresses

on maximum shearing stress of a Hertzian contact and (b) determine the magnitude of the effects of press fit and centrifugal force on roller bearing life.

ANALYSIS

Current evaluations of rolling-element fatigue life are based on either the orthogonal shear stress or the maximum shearing stress (ref. 6) which occur in a zone under the rolling-element contact surfaces. These shearing stresses are a function of the contact (Hertz) stress due to two bodies in contact. The Hertzian stress, in turn is a function of load, geometry, and material physical properties of the rolling-element bodies. Jones (ref. 7), based on the work of Thomas and Hoersch (ref. 8) shows the principal stresses (fig. 1) due to a Hertzian loading to be:

$$\frac{\Lambda X_x}{b} = -2\delta\left[\sqrt{1 + \left(\frac{Z}{b}\right)^2} - \frac{Z}{b}\right] \tag{1}$$

$$\frac{\Lambda Y_Y}{b} = -\frac{\left[\sqrt{1 + \left(\frac{Z}{b}\right)^2} - \frac{Z}{b}\right]^2}{\sqrt{1 + \left(\frac{Z}{b}\right)^2}} \tag{2}$$

$$\frac{\Lambda Z_Z}{b} = -\frac{1}{\sqrt{1 + \left(\frac{Z}{b}\right)^2}} \tag{3}$$

By letting $u = Z/b$ and $t = \sqrt{1 + u^2}$, these equations become

$$\frac{\Lambda X_x}{b} = -2\delta\,(t - u) \tag{4}$$

$$\frac{\Lambda Y_Y}{b} = \frac{-(t - u)^2}{t} \tag{5}$$

$$\frac{\Lambda Z_Z}{b} = -\frac{1}{t} \tag{6}$$

For roller bearings, the maximum shear stress is determined by the principal stresses in the Z (direction of Hertzian loading) and the Y (direction of rolling) direction. Thus

$$\tau = \frac{1}{2}\,(Z_Z - Y_Y) \tag{7}$$

So, for Hertzian loading only, substituting from Eqs. (2) and (3) into equation (7) gives

$$\tau = \frac{b}{\Lambda}\left(t - u - \frac{1}{t}\right) \tag{8}$$

But, from reference 7,

$$b^2 = \frac{P'_o (\theta_a + \theta_b)}{\pi \ell \rho} \tag{9}$$

$$\theta_a = \frac{4(1 - \delta_a^2)}{E_a} \tag{10}$$

$$\theta_b = \frac{4(1 - \delta_b^2)}{E_b}$$

$$\Lambda = \left[\frac{1 - \delta_a^2}{E_a} + \frac{1 - \delta_b^2}{E_b} \right] \frac{2}{\Sigma \rho} \tag{11}$$

and

$$S_{max} = \frac{2 P'_o}{\pi \ell b} \tag{12}$$

Now, let

$$E' = \frac{1 - \delta_a^2}{E_a} + \frac{1 - \delta_b^2}{E_b} \tag{13}$$

then

$$\theta_a + \theta_b = 4E' \tag{14}$$

$$\Lambda = \frac{2E'}{\Sigma \rho} \tag{15}$$

Equation (9) can now be written

$$b = \left(\frac{2 P'_o}{\pi \ell b} \right) \left(\frac{2E'}{\sqrt{\rho}} \right) \tag{16}$$

or

$$b = S_{max} \Lambda \tag{17}$$

Substituting equation (17) into equation (8) gives

$$\tau = S_{max} \left(t - u - \frac{1}{t} \right) \tag{18}$$

Thus, the shear stress, made nondimensional by the maximum Hertz stress, is a direct function of u, the depth below the surface, as shown in figure 2. A maximum value of the maximum shear stress occurs at a depth (u) of approximately 0.78. By taking the derivative of equation (18) with respect to u and setting the result equal to zero, one obtains

$$\frac{d\tau}{du} = S_{max} \left(\frac{u}{t} + \frac{u}{t^3} - 1 \right) = 0 \tag{19}$$

The solution to equation (19) is $u = 0.786152$, and the corresponding equation for the maximum shear stress becomes

$$\tau_{max} = - 0.30028\ S_{max} \tag{20}$$

Equations (18) and (20) account for the subsurface stresses due only to the Hertzian contact and do not account for the effects of press fitting an inner ring on a shaft or for the effects of inner-ring speed. These effects can be accounted for, using the method of superposition, by determining the values of subsurface stress in the Z and Y direction as a function of depth below the surface to correspond with equations (5) and (6).

Stress Due to Press Fit

From reference 9 we can write, for the hoop stress

$$(\sigma_h)_{PF} = \frac{1}{r_o^2 - r_i^2} \left[r_i^2 P_i - r_o^2 P_o + \left(\frac{r_i r_o}{r}\right)^2 (P_i - P_o) \right] \tag{21}$$

Note that $P_o = 0$ and that P_i is due to a press fit of the ring on a shaft, that is,

$$P_i = \frac{\Delta}{r_i K_1} \tag{22}$$

Equation (21) can be written

$$(\sigma_h)_{PF} = \frac{P_i r_i^2}{r_o^2 - r_i^2} \left[1 + \left(\frac{r_o}{r}\right)^2 \right] \tag{23}$$

Similarly, we can write, for the radial stress

$$(\sigma_r)_{PF} = \frac{P_i r_i^2}{r_o^2 - r_i^2} \left[1 - \left(\frac{r_o}{r}\right)^2 \right] \tag{24}$$

If we let

$$\frac{r_i}{r_o} = B \quad \text{and} \quad \frac{r}{r_o} = y \tag{25}$$

Equations (23) and (24) become

$$(\sigma_h)_{PF} = \frac{P_i B^2}{1 - B^2} \left(1 + \frac{1}{y^2} \right) \tag{26}$$

$$(\sigma_r)_{PF} = \frac{P_i B^2}{1 - B^2}\left(1 - \frac{1}{y^2}\right) \tag{27}$$

Stresses Due to Inner Ring Speed

From reference 9 we can write, for the hoop stress,

$$(\sigma_h)_{CF} = \frac{3 - 2\upsilon}{8(1 - \upsilon)}\left(\frac{\gamma\omega^2}{g}\right)\left[r_o^2 + r_i^2 + \left(\frac{r_o r_i}{r}\right)^2 - r^2\left(\frac{1 - 2\upsilon}{3 - 2\upsilon}\right)\right] \tag{28}$$

Similarly, for the radial stress

$$(\sigma_r)_{CF} = \frac{3 - 2\upsilon}{8(1 - \upsilon)}\left(\frac{\gamma\omega^2}{g}\right)\left[r_o^2 - r_i^2 - r^2 - \left(\frac{r_o r_i}{r}\right)^2\right] \tag{29}$$

let

$$K = \left(\frac{3 - 2\upsilon}{8(1 - \upsilon)}\right)\left(\frac{\gamma}{g}\right), \quad G = \frac{1 - 2\upsilon}{3 - 2\upsilon} \tag{30}$$

and using equation (25), equations (28) and (29) become

$$(\sigma_h)_{CF} = K\omega^2 r_o^2\left[1 + B^2 + \frac{B^2}{y^2} - Gy^2\right] \tag{31}$$

$$(\sigma_r)_{CF} = K\omega^2 r_o^2\left[1 - B^2 - \frac{B^2}{y^2} - y^2\right] \tag{32}$$

Combined Stresses

By the method of superposition, the principal stresses in the Z and Y directions become

$$S_Z = Z_Z + (\sigma_r)_{PF} + (\sigma_r)_{CF} \tag{33}$$

$$S_y = Y_Y + (\sigma_h)_{PF} + (\sigma_h)_{CF} \tag{34}$$

and the maximum shear stress is

$$\tau = \frac{1}{2}(S_Z - S_y) \tag{35}$$

To utilize these equations, however, one must determine the relation between u and y so that the stresses can all be determined at the same location.

From geometry, (figs. (1) and (3))

$$r = r_o - Z = r_o - ub \tag{36}$$

or

$$\frac{r}{r_o} = 1 - \frac{ub}{r_o} = y \tag{37}$$

and

$$u = \frac{r_o}{b}(1 - y) \tag{38}$$

Substituting equation (17) gives

$$u = \frac{r_o}{S_{max}\,\Lambda}(1 - y) \tag{39}$$

From figure (3)

$$\Sigma\rho = \frac{1}{r_o} + \frac{1}{R_r} = \frac{R_r + r_o}{r_o R_r} \tag{40}$$

Substituting equation (40) into equation (15) gives

$$\Lambda = \frac{2E'\, r_o R_r}{r_o + R_r} \tag{41}$$

Using equation (41) in equation (39) lets us write

$$u = \frac{\left(\frac{r_o}{R_r} + 1\right)}{2S_{max}\,E'}(1 - y) \tag{42}$$

or

$$u = \frac{R' + 1}{2S_{max}E'}(1 - y) \tag{43}$$

where

$$R' = \frac{r_o}{R_r} \tag{44}$$

For simplicity, let

$$K_2 = \frac{R' + 1}{2S_{max}E'} \tag{45}$$

then

$$u = K_2(1 - y) \tag{46}$$

Proper substitution of equations (33) and (34) into equation (35) using equations (5), (6), (26), (27), (31), and (32) along with equation (17) leads to the following expression for the maximum shear stress as a function of depth below a Hertzian contact, accounting for both ring press fit and ring speed.

$$\tau = S_{max}\left(t - u - \frac{1}{t}\right) - (m + AB^2)\left(\frac{1}{y^2}\right) + \frac{A}{2}(G - 1)y^2 - AB^2 \qquad (47)$$

where, for simplicity

$$m = \frac{P_i B^2}{1 - B^2}$$
$$A = K\omega^2 r_o^2 \qquad (48)$$

Again, taking the derivative of equation (47) with respect to y and setting the result equal to zero leads to the value of y where the shear stress is a maximum. Using the chain rule that $ds/dy = ds/du \cdot du/dy$,

$$\frac{d\tau}{dy} = -S_{max}K_2\left[\frac{u}{t} + \frac{u}{t^3} - 1\right] + \frac{2(m + AB^2)}{y^3} + A(G - 1)y = 0 \qquad (49)$$

Using the Lundberg-Palmgren (ref. 10) analysis where

$$L = \left(\frac{K_3 Z_o^h}{\tau_{max}^c V}\right)^{1/e} \qquad (50)$$

where Z_o is the depth to the maximum value of the maximum shearing stress from equation (49) and τ_{max} is its value from equation (47), the effect of the press fits and centrifugal force on inner race life can be determined. The effects of press fit would not, however, affect the life of the outer race. However, centrifugal loading of the rollers on the outer race does affect the outer race life which can be readily determined. Knowing the life of the inner and outer raceways, the life of the bearing can be determined from Lundberg-Palmgren (ref. 10) as follows:

$$\frac{1}{L^e} = \frac{1}{L_i^e} + \frac{1}{L_o^e} \qquad (51)$$

RESULTS AND DISCUSSION

Inner-Race Life

The relative values of subsurface stress are shown in figure 4 for the typical roller bearing inner-ring data given in table I. The principal stress in the Z-direction is shown in figure 4(a) while the principal stress in the

Y-direction is shown in figure 4(b). The stress values have been nondimensionalized by the Hertz stress (S_{max}). Note that $y = 0.90$ is the inner radius and $y = 1$ is the outer radius of the ring.

In figure 4(a), the stress due to ring speed is the largest component at the inner surface, but the subsurface compressive stress due to the Hertzian loading becomes dominant as the outer (contact) surface is approached. In figure 4(b), the stress due to ring speed is again the largest at the inner surface and the stress from the press fit is influential. Note that the ring speed is high in the example problem and that the pressure assumed for the press fit is probably moderate. However, the compressive stress due to the Hertzian loading becomes dominant as the outer surface is approached. The principal stress Sy does remain tensile (positive) until about $y = 0.995$, which will influence the maximum shear stress.

When the principal stresses from Fig. 4 are combined in accordance with equation (35) the result is the maximum shear stress, shown in figure 5. To observe the change in the maximum shear stress when the effects of ring press fit and ring speed are added, one needs to compare the results in figure 5 with those due to Hertzian loading only (fig. 2). This is shown in figure 6, where the contributions to the maximum shear stress are shown separately. The increase in maximum value of the maximum shear stress for this example shown is about 33 percent. The solution to equation (49) for this example is $y_{max} = 0.998204$, where $\tau_{max} = -0.402\ S_{max}$. The depth to the maximum shear stress changed only very slightly from that of the Hertz loading only.

The rolling-element fatigue life is taken to be inversely proportional to the maximum shear stress to the ninth power (ref. 10). Therefore, if we define a life ratio LR as the ratio of fatigue life based on the maximum shear stress that included the effects of ring speed and press fit to the fatigue life based on the maximum shear stress from the Hertzian loading only, we could write

$$LR = \frac{L_T}{L_H} = \left[\frac{\tau_{max,H}}{\tau_{max,T}}\right]^9 \tag{52}$$

where $\tau_{max,H}$ is obtained from equation (20) and $\tau_{max,T}$ is obtained from equation (47), using the value of y obtained from equation (49). The value of LR, which is a measure of the effects of a press fit and ring speed, for the example is

$$LR = \left(\frac{-\ 0.30028\ x\ 1.4x10^9}{-\ 0.40167\ x\ 1.4x10^9}\right)^9 = 0.0729$$

That is, the corrected life is only 0.07 times that calculated using stresses from the Hertzian loading only.

To observe these effects over a broader range of variables, equations (47) and (49) were used to calculate the life ratio LR (eq. (52)) for ring thicknesses (B) from 0.5 to 0.92, for Hertz stresses from $0.69x10^9$ to $2.07x10^9$ N/M^2 (100 000 to 300 000 psi) using ring speeds of 500 and 2000 rad/sec, for rings with an outer radius of 25.4 and 63.5 mm (1 and 2.5 in.), at a press fit pres-

sure of 6.9×10^6 N/M^2 (1000 psi), and with a radius ratio R' of both 5 and 10. The results are shown in figures 7 to 10.

Figure 7, for a ring with an outer radius of 63.5 mm (2.5 in.) shows that the relative influence of press fit and ring speed on fatigue life diminishes as the Hertz stress is increased, or as the ring becomes thicker, or as the ring speed is decreased. Figure 8 shows the same data plotted against radius ratio. Several calculations for the conditions of figure 7 were made with $R' = 5$ and the life ratio results were the same. Increasing the press fit pressure would lower the values of LR. The pressure used in figures 7 and 8 represent an interference fit of about 0.051 mm (0.002 in.) on the diameter.

Figures 9 and 10 show the results obtained for an outer radius of 25.4 mm (1.0 in.) and an R' of 5. The life ratio results with an R' of 10 were the same. A comparison of figures 7 and 9 shows that the life ratios with the smaller outer radius were generally higher than for the corresponding larger ring, and were not so influenced by ring speed.

Since there are many values of LR of 0.5 or less, it may be concluded that the press fit and loading due to ring speed can have a significant effect on the fatigue life calculated for an inner-ring contact.

Roller Bearing Life

Using equations (50) and (51) the life of the entire bearing can be determined. These results are shown in nondimensional form in figure 11(a). For a bearing without any centrifugal force or press fit effects the normalized life is one. Considering the effects of centrifugal force alone, the relative life at approximately 1.2 million DN is approximately 60 percent the life using a straight Lundberg-Palmgren calculation of bearing catalog life. At the same speed, considering press fit alone, the life is also approximately 60 percent of the catalog calculation. However, both effects in combination produce a life of approximately 40 percent of the catalog calculation.

These effects at higher speeds are more dramatic. As an example, at approximately 3 million DN, the effect of press fit is lessened to produce a life of approximately 85 percent the catalog life. The effects of centrifugal force only produce a life of approximately 10 percent the catalog life. However, in combination, these effects can produce a life of only 8 or 9 percent the bearing catalog life.

Effect of Mean Stress

Lundberg-Palmgren (eq. (50)) in their original analysis considered only the maximum value of the reverse orthogonal shearing stress (ref. 10). Metallurgical studies of rolling-element specimens which failed in surface fatigue have shown, based upon crack propagation, that the critical shearing stresses can be the orthogonal, the octahedral or the maximum shear stress. All these shear stresses are a function of the maximum Hertzian (contact) stress. For the calculations performed herein the values of the maximum shear stress were used in equation (50) to determine bearing life. For a given Hertzian stress and with the addition of hoop stresses due to press fits and centrifugal force, the mean value of the shear stress will increase. However, the amplitude of

the maximum shear stress will remain unchanged. For a given operating condition, the hoop stresses impose a steady or static stress. The steady or static stress define the minimum shear stress. The maximum value of shear stress equals the amplitude of the maximum shear stress plus the static stress. The mean stress can be defined as the average of these two values.

A Goodman diagram type approach may be an effective but untried method to account for the effect of mean stress in rolling-element fatigue. Referring to figure 12, there is shown a proposed Goodman type diagram based upon the maximum shear stress amplitude τ_a and the mean shear stress, τ_m. For the calculations of figure 12, the amplitude of the maximum shear stress τ_a on the bearing inner race was 0.39×10^9 N/M^2 (56 100 psi). The mean value τ_m would be 0.19×10^9 N/M^2 (28 050 psi). From reference 11, the value of the fracture stress Su for AISI 52100 or AISI M-50 can be taken as 2.34×10^9 N/M^2 (340 000 psi). Based upon these values the effective maximum shear stress τ_e from figure 12 would be approximately 0.42×10^9 N/M^2 (61 144 psi) based upon the following proposed equation for a Goodman diagram.

$$\tau_e = \frac{\tau_a \cdot \tau_m}{S_u - \tau_m} + \tau a = \frac{\tau_a}{1 - \left(\frac{\tau_m}{S_u}\right)} \qquad (53)$$

The values of τ_e from equation (53) can be used in equations (50) and (51) as the value of τ_{max} to predict bearing life. This was done for the data of figure 11(a), the results of which are shown in figure 11(b). The results of the analysis indicated bearing lives for the conditions shown ranging from 70 to 80 percent of those lives where there are no effects of hoop stresses due to centrifugal force and press fits. These lives contrast with those predictions shown for comparison in figure 11(b) based upon only considering the maximum shear stress τ_{max} as a result of hoop stress without considering the effect of mean shear stress. It becomes apparent that the reduction in lives predicted using a value of τ_e from a Goodman diagram which considers hoop stresses is less significant than using the resultant value of the maximum shear stress, τ_{max}. Experimental research needs to be performed to verify and refine this approach.

SUMMARY

An analysis was performed to determine the effects of inner-ring speed and press fits on roller bearing fatigue life. The effects of the resultant hoop and radial stress on the principal stresses were considered. The maximum shear stresses below the Hertzian contact were determined for different conditions of inner-ring speed and load and were applied to a conventional roller bearing life analysis. The effect of mean stress was determined using a Goodman diagram approach. The following results were obtained.

1. Hoop stresses caused by press fits and centrifugal force can reduce bearing life by as much as 90 percent.

2. Use of a Goodman diagram calculation considering mean maximum shear stress and shear stress amplitude to determine an effective maximum shear stress resulted in the calculation of roller bearing life 20 to 30 percent less than theoretical life predictions.

3. The depth to the maximum shear stress remains relatively unchanged by speed and press fit, over the range calculated, from that established by conventional theory.

REFERENCES

1. Scott, R.L.; Kepple, R.K., and Miller, M.H., "The Effect of Processing-induced Near-surface Residual Stress on Ball Bearing Fatigue," Rolling Contact Phenomena, J.B. Bidwell, Ed., Elsevier, 1962, pp. 301-316.

2. Zaretsky, E.V., Parker, R.J., Anderson, W.J., and Miller, S.T., "Effect of Component Differential Hardnesses on Residual Stress and Rolling-Contact Fatigue," NASA TN-D-2664, 1965.

3. Alman, J.O.: Effects of Residual Stress on Rolling Bodies. Rolling Contact Phenomena, J.B. Bidwell, Ed. Elsevier, 1962, pp. 400-424.

4. Townsend, D.P., and Zaretsky, E.V., "Effect of Shot Peening on Surface Fatigue Life of Carburized and Hardened AISI 9310 Spur Gears," NASA TP-2047, Aug. 1982.

5. Czyzewski, T., "Influence of a Tension Stress Field Introduced in the Elastohydrodynamic Contact Zone on Rolling-Contact Fatigue," Wear, Vol. 34, pp. 201-214, 1975.

6. Harris, T.A., Rolling Bearing Analyses, John Wiley and Sons, Second Edition, NY, 1984.

7. Jones, A.B., "Analysis of Stress and Deflections," Vol. I, New Departure Div., General Motors Corp, 1946.

8. Thomas, H.R., and Hoersch, V.A., Stresses due to the Pressure of One Elastic Solid on Another," Bulletin of Engineering Experiment Station No. 212, University of Illinois, 1930.

9. Faupel, J.H.: Engineering Design. John Wiley and Sons, Inc. 1964.

10. Lundberg, G.; and Palmgren, A., "Dynamic Capacity of Rolling Bearings," Acta Polytech. Scand, Mech. Engr. Ser., Vol. 1, no. 3, 1947.

11. Sachs, G., Sell, R., and Brown, W.F., Jr., "Tension, Compression, and Fatigue Properties of Several Steels for Aircraft Bearing Applications, Trans. ASTM, 1959, pp. 1-23.

TABLE I. - VALUES FOR EXAMPLE PROBLEM

Variables	
B	0.90
P_1	6.89×10^6 N/M^2 (1000 psi)
ω	2000 rad/sec
r_o	63.5 mm (2.5 in.)
R'	10
S_{max}	1.379×10^9 N/M^2 (200 000 psi)
Constants	
K for steel	3352 N-sec^2/M^4 (3.14×10^{-4} lb-sec^2/in.^{4})
G	0.1667
E'	9.11×10^{-12} M^2/N (6.28×10^{-8} in.^{2}/lb)

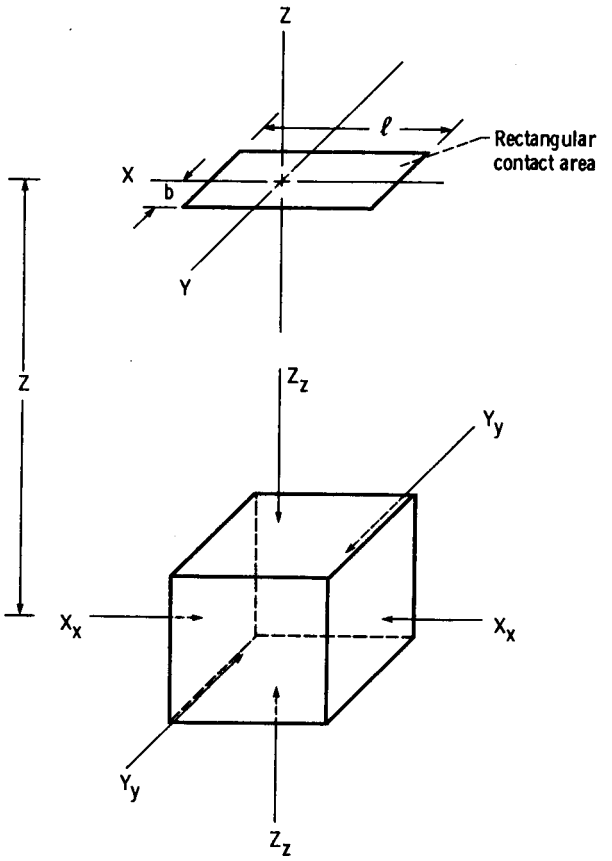

Figure 1. - Principal stresses on elementary subsurface particle at depth Z under Hertzian pressure area.

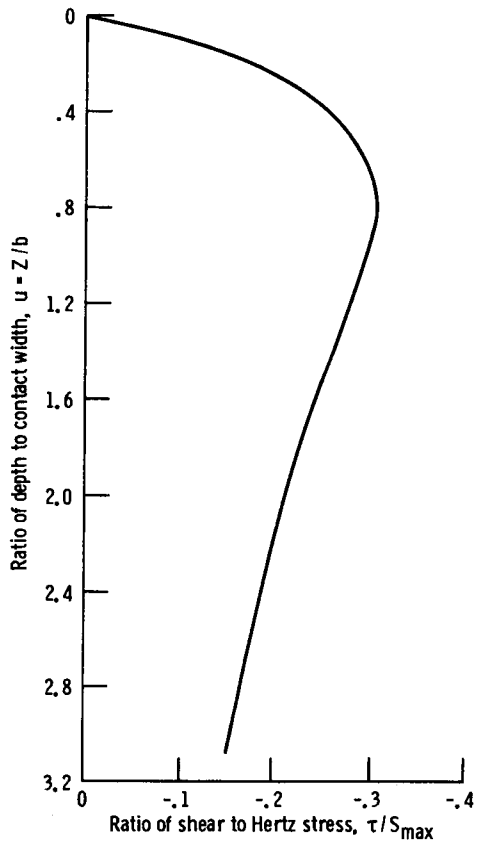

Figure 2. - Maximum shear stress as a function of depth below the surface, for Hertzian loading. Stress on Z-axis, below rectangular pressure area.

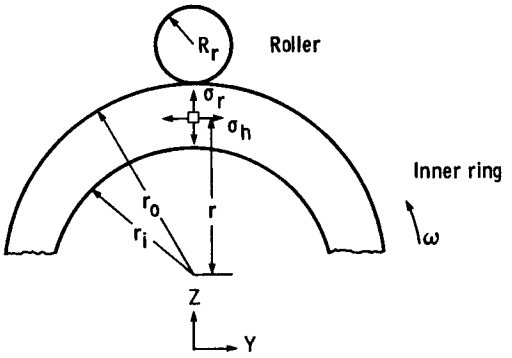

Figure 3. - Definition of additional terms used in analysis of subsurface stress in roller bearing inner ring.

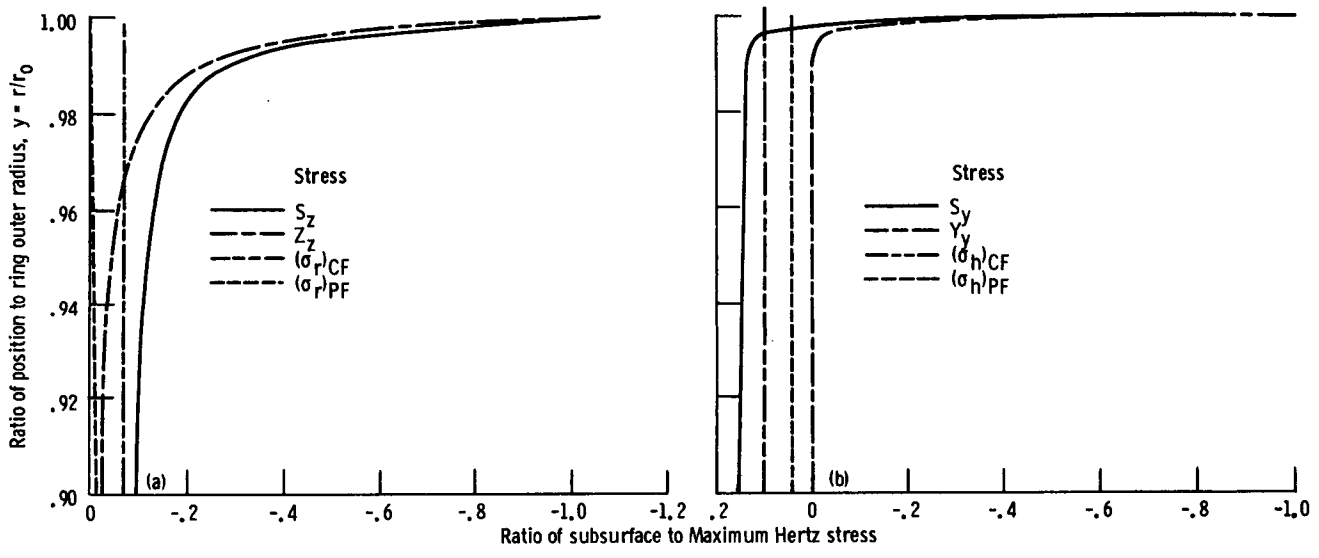

(a) In Radial, or Z-direction.

(b) Hoop, or Y-direction.

Figure 4. - Components of subsurface stress in roller bearing inner ring, for conditions described in Table I.

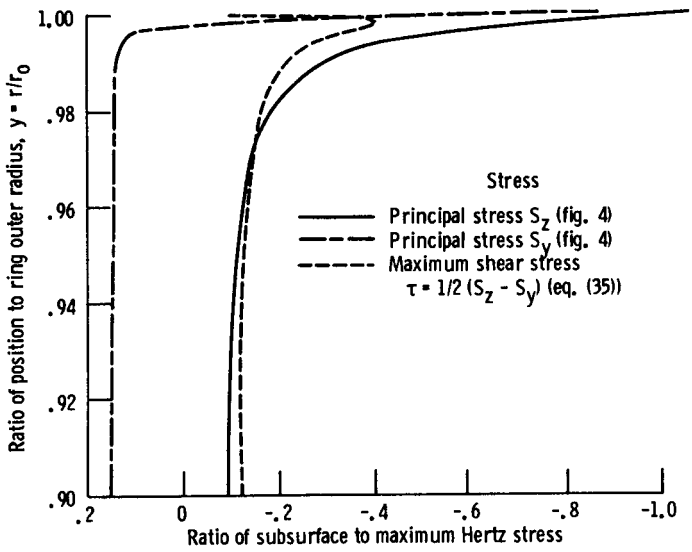

Figure 5. -Principal and maximum shear stresses in roller bearing inner ring, for conditions described in Table I.

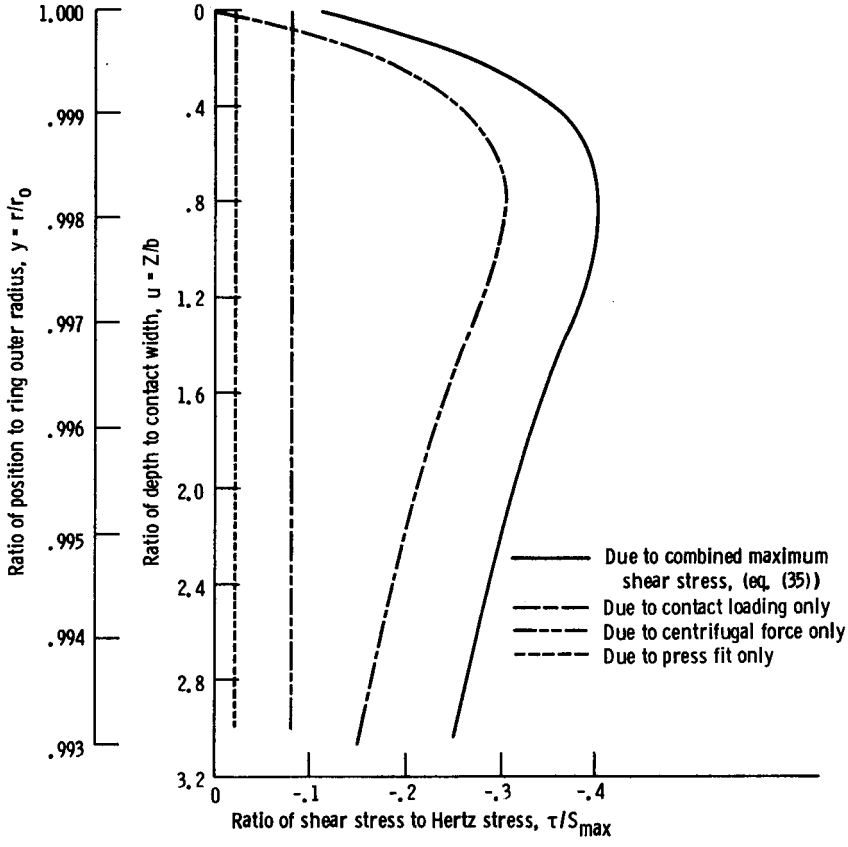

Figure 6. - Components of combined maximum shear stress in roller bearing inner ring, for conditions described in Table I.

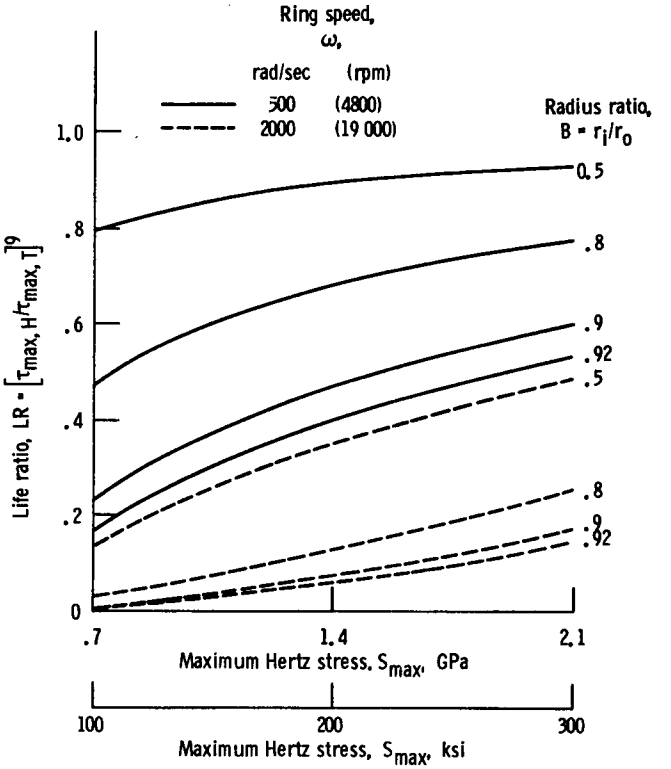

Figure 7. - Life ratio as a function of Hertz stress, for several ring thicknesses, at two ring speeds. r_o = 63.5 mm (2.5 in.), P_i = 6.0x10^6 N/m^2 (1000 psi) R' = 10.

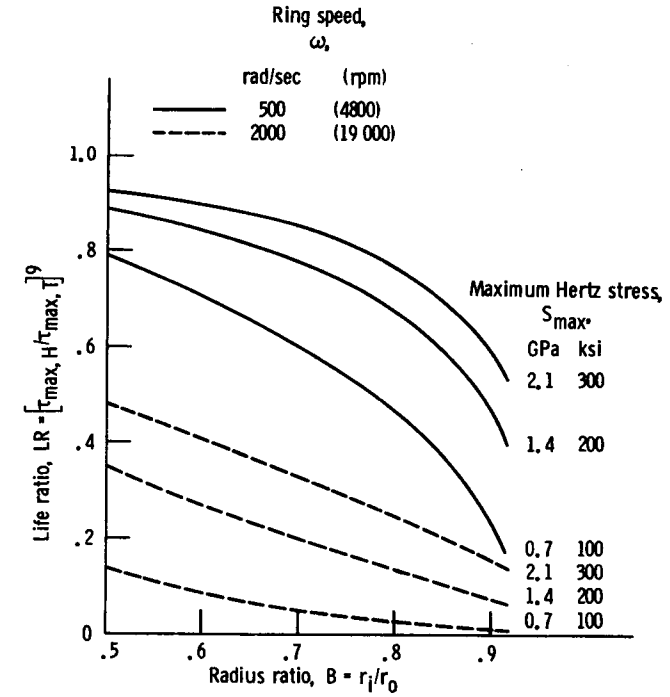

Figure 8. - Life ratio as a function of radius ratio for three values of maximum Hertz stress, at two ring speeds. r_o = 63.5 mm (2.5 in.), P_i = 6.9x10^6 N/m^2 (1000 psi), R' = 10.

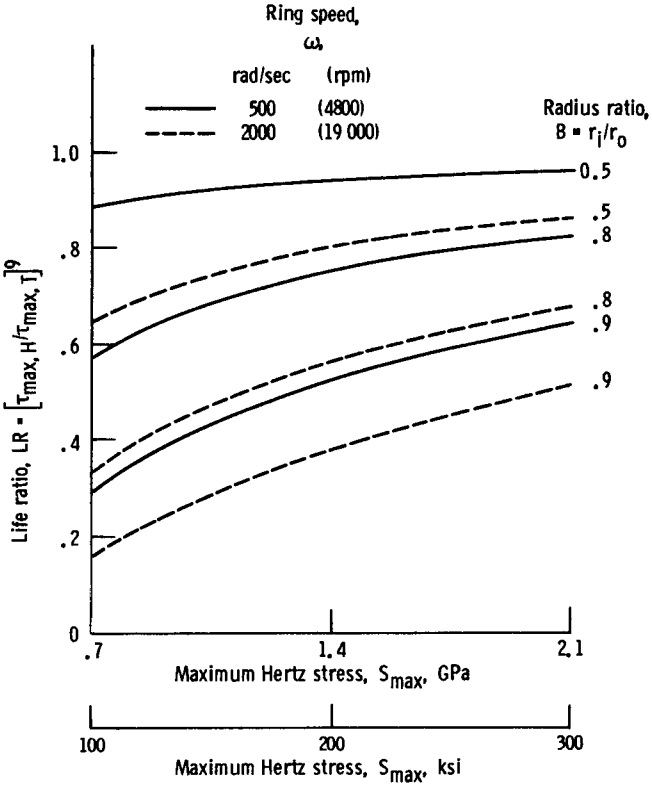

Figure 9. - Life ratio as a function of Hertz stress, for three ring thicknesses and two ring speeds. r_o = 25.4 mm (1.0 in.), P_i = 6.9x10^6 N/m^2 (1000 psi), R' = 5.

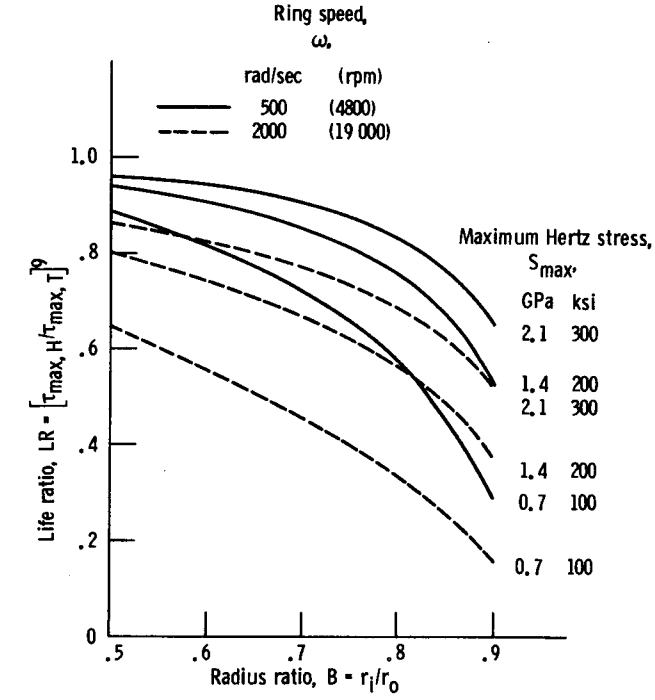

Figure 10. - Life ratio as a function of radius ratio for three values of Hertz stress, at two ring speeds. r_o = 25.4 mm (1.0 in.), P_i = 6.9x10^6 N/m^2 (1000 psi), R' = 5.

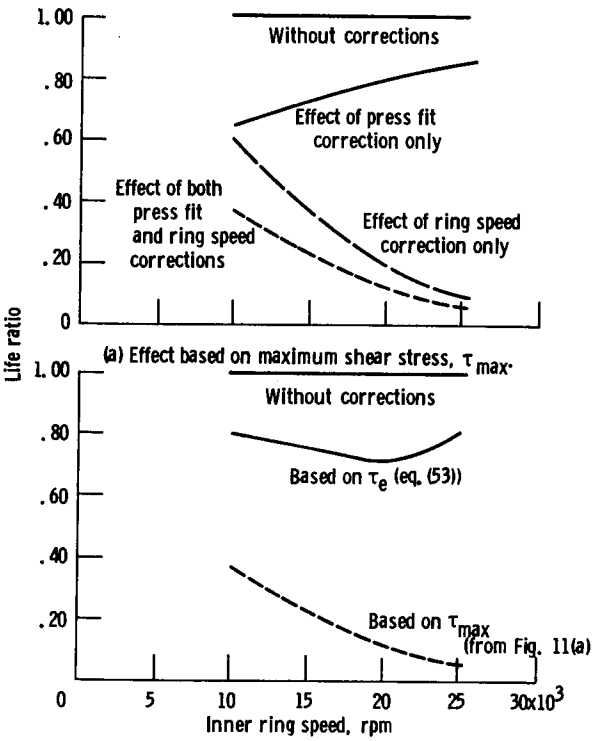

(b) Effect of both press fit and ring speed life corrections based on τ_e and τ_{max}.

Figure 11. - Effect of hoop stresses on the fatigue life of 118-mm bore roller bearing. Radial load 8900 N (2000 lb). Interference fit pressure 6.89x10^6 N/m^2 (1000 psi). Maximum Hertz stress at maximum loaded roller 1290 N/m^2 (187 000 psi).

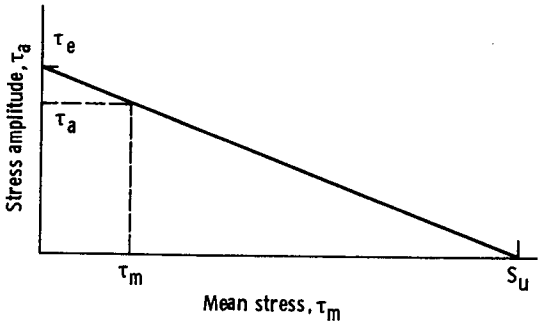

Figure 12. - Proposed Goodman diagram for rolling-element fatigue life predictions to account for effects of hoop stresses.

1. Report No.	2. Government Accession No.	3. Recipient's Catalog No.
NASA TM-87165		

4. Title and Subtitle	5. Report Date
Effect of Interference Fits on Roller Bearing Fatigue Life	January 1986
	6. Performing Organization Code: 505-33-7C

7. Author(s)	8. Performing Organization Report No.
Harold H. Coe and Erwin V. Zaretsky	E-2516
	10. Work Unit No.

9. Performing Organization Name and Address	11. Contract or Grant No.
National Aeronautics and Space Administration Lewis Research Center Cleveland, Ohio 44135	
	13. Type of Report and Period Covered: Technical Memorandum

12. Sponsoring Agency Name and Address	14. Sponsoring Agency Code
National Aeronautics and Space Administration Washington, D.C. 20546	

15. Supplementary Notes

16. Abstract

An analysis was performed to determine the effects of inner-ring speed and press fits on roller bearing fatigue life. The effects of the resultant hoop and radial stresses on the principal stresses were considered. The maximum shear stresses below the Hertzian contact were determined for different conditions of inner-ring speed and load, and were applied to a conventional roller bearing life analysis. The effect of mean stress was determined using a Goodman diagram approach. Hoop stresses caused by press fits and centrifugal force can reduce bearing life by as much as 90 percent. Use of a Goodman diagram predicted life reductions of 20 to 30 percent. The depth of the maximum shear stress remained virtually unchanged.

17. Key Words (Suggested by Author(s))	18. Distribution Statement
Fatigue; Rolling bearings; Stress analysis; Life analysis	Unclassified - unlimited STAR Category 37

19. Security Classif. (of this report)	20. Security Classif. (of this page)	21. No. of pages	22. Price*
Unclassified	Unclassified		

*For sale by the National Technical Information Service, Springfield, Virginia 22161